ELASTOPLASTIC CONTACT CONDUCTANCE MODEL FOR ISOTROPIC CONFORMING ROUGH SURFACES AND COMPARISON WITH EXPERIMENTS

M.R. Sridhar* and M.M. Yovanovich†
Microelectronics Heat Transfer Laboratory
Department of Mechanical Engineering
University of Waterloo
Waterloo, Ontario, Canada N2L 3G1

ABSTRACT

A new thermal elastoplastic contact conductance model for isotropic conforming rough surfaces is proposed. This model is based on surface and thermal models used in the Cooper, Mikic and Yovanovich plastic model, but it differs in the deformation aspects of the thermal contact conductance model. The model incorporates the recently developed simple elastoplastic model for sphere-flat contacts, and it covers the entire range of material behavior: i.e., elastic, elastoplastic and fully plastic deformation. Previously data were either compared with the elastic model or the plastic model assuming a type of deformation *a priori*. The model is used to reduce previously obtained isotropic contact conductance data which cover a wide range of surface characteristics and material properties. For the first time data can be compared with both the elastic and plastic models on the same plot. This model explains the observed discrepancies noted by previous workers between data and the predictions of the elastic or plastic models.

NOMENCLATURE

A_a	=	apparent contact area, m^2
$\tilde{A}$	=	contact area for a single circular contact, m^2
A_r	=	real contact area, m^2
a	=	mean circular contact radius, m
c_1, c_2	=	Vickers correlation coefficients, c_1, MPa
d_V	=	Vickers indentation diagonal, μm
E	=	elastic modulus, MPa
E'	=	equivalent elastic modulus, MPa $\equiv \left[(1-\nu_A^2)/E_A + (1-\nu_B^2)/E_B\right]^{-1}$
$\tilde{F}$	=	load on a single circular contact (sphere-flat), N
$f_{ep}(\epsilon_c^*)$	=	function used in the elastoplastic model, Eq. (27)
H_e	=	elastic contact hardness, MPa
$H_{c\ or\ p}$	=	plastic contact hardness, MPa
H_{ep}	=	elastoplastic contact hardness, MPa
h_c	=	contact conductance, Eqs. (1) & (41)
k_s	=	harmonic mean thermal conductivity, $\equiv 2k_Ak_B/(k_A+k_B)$, $W/m\cdot K$
m	=	effective mean absolute surface slope, $\equiv \sqrt{m_A^2+m_B^2}$, rad
n	=	contact spot density, m^{-2}

*Graduate Research Assistant
†Professor and Director, Fellow ASME

P = nominal contact pressure, MPa

Q = heat transfer rate, W

S_f = material yield or flow stress, MPa

T_c = mean interface temperature, $^\circ C$

Y = surface mean plane separation, m

Greek Symbols

β = radius of curvature of asperity summits, m

ΔT_c = effective temperature drop across the interface, $^\circ C$

δ = contact displacement, m

ϵ_c^* = non-dimensional contact strain, $\equiv \frac{E'}{S_f} \cdot \frac{a}{\beta}$ or $\frac{E'}{S_f} \cdot \sqrt{\frac{\delta}{\beta}}$ or $1.67 \cdot \frac{E'}{S_f} \cdot m$

λ = dimensionless surface mean plane separation, $\equiv Y/\sigma$

ν = Poissons ratio

σ = RMS surface roughness heights for given surface or surface pair, $\equiv \sqrt{\sigma_A^2 + \sigma_B^2}$, m

Subscripts

A, B = surfaces A and B

a = apparent area or based on contact radius (a)

c = contact or plastic

e = elastic

p = plastic

ep = elastoplastic

r = real

Abbreviations

BGT = Bush, Gibson and Thomas

CMY = Cooper, Mikic and Yovanovich

GW = Greenwood and Williamson

Ni = Nickel

SS = Stainless Steel

WA = Whitehouse and Archard

Zr-Nb = Zirconium alloy with Niobium

Zr-4 = Zirconium alloy

INTRODUCTION

The thermal contact conductance models for two conforming rough surfaces consist of three basic models: the thermal model, the surface model and the deformation model. The essential difference between the different contact conductance models is found in the surface model. Most of the contact conductance models for isotropic surfaces assume circular contact spots and use either the Hertz elastic model [Johnson (1985)] or the geometric plastic deformation model. Depending on the type of deformation model used the contact conductance model for conforming rough surfaces becomes an elastic or a plastic model.

There is a considerable confusion regarding the type of deformation associated with a pair of contacting conforming rough surfaces under static load. In order to predict experimental results with the present contact conductance models a type of deformation must be assumed *a priori*. A plasticity index has been used to assess the type of deformation (elastic or plastic). This index requires a value of plastic hardness. Since only bulk hardness values were used instead of an appropriate microhardness it did not neccessarily point to the right deformation mode.

There is a need to be able to reduce data without assuming a type of deformation. This is because most of the rough surfaces in contact under load undergo elastoplastic deformation. This can be achieved by incorporating an elastoplastic deformation model into the present thermal contact conductance model.

Recently a simple elastoplastic model for sphere-flat contacts has been proposed by Sridhar and Yovanovich (1994). This model predicts the contact radius or displacement for all three regimes of deformation: elastic, elastoplastic and fully plastic.

Sridhar and Yovanovich (1993b) have incorporated the explicit form of this elastoplastic deformation model into a thermal constriction resistance model for sphere-flat contacts and they were able to predict experimental

results for a variety of metals (Keewatin tool steel, Ni200 and Carbon steel) quite accurately.

The aim of the present paper is to develop a novel thermal contact conductance model for conforming rough isotropic surfaces using the recently proposed elastoplastic model for sphere-flat contacts and then reduce experimental data [Antonetti (1983) and Hegazy (1985)] obtained for similar metal pairs to dimensionless form using this model. Data reduced using the elastoplastic model can be compared with both the elastic and plastic models on the same plot.

BRIEF REVIEW OF CONTACT CONDUCTANCE MODELS

There are a number of thermal contact conductance models available in the literature. The important models which use statistical analysis are: i) Greenwood and Williamson (1966) (GW) model, ii) Cooper, Mikic and Yovanovich (1969) (CMY) and Mikic (1974) model, iii)Bush, Gibson and Thomas (1975) (BGT) asymptotic model and iv) Whitehouse and Archard (1970) (WA) model. A detailed review of these contact conductance models can be found in Sridhar and Yovanovich (1993a). In order to reduce experimental data with the new elastoplastic model the surface microhardness distribution of the softer material in contact is required. Since only isotropic data sets from Antonetti (1983) and Hegazy (1985) have these distributions in the form of an experimental correlation between the Vickers microhardness and the indentation size ($H_V = c_1 {d_V}^{c_2}$), only data sets from these two sources will be used.

Elastic-Plastic models for contacting rough surfaces have been proposed in the past by Ishigaki et al. (1979), Chang et al. (1987) and Majumdar and Bhushan (1991). The Ishigaki et al. (1979) model assumes that the total deformation is the sum of elastic and plastic deformations. Chang et al. (1987) have improved upon the previous models by considering volume conservation of an asperity control volume during plastic deformation. The Majumdar and Bhushan (1991) model is based on the contact mechanics of two fractal surfaces in contact. The ability of the above models to predict experimental data for a single asperity contact in the elastoplastic regime is not clear. Hence in the present work a simple model for sphere-flat contact proposed by Sridhar and Yovanovich (1994) will be used. This simple model has been shown to predict quite well experimental data [Foss and Brumfield (1922), Tabor (1951) and Fisher (1985)] for sphere-flat contacts in the elastoplastic regime.

There is a choice of converting any of the surface models (CMY/Mikic, GW, WA and BGT) into an elastoplastic model. We know that the GW-model and the WA-model require an additional surface parameter [see Sridhar and Yovanovich (1993a)] and the BGT model is only an approximate model which does not compare well with the other models. Hence the present work of developing an elastoplastic model for isotropic conforming rough surfaces will be based on the existing, well-established, CMY plastic model and the Mikic elastic model which followed from the CMY plastic model. The main results from the analyses of the CMY plastic model and the Mikic elastic model are given in Table 1 and Table 2. The thermal model used in these contact conductance models was first presented by Cooper, Mikic and Yovanovich (1969) and in a convenient form by Yovanovich (1982), where the contact conductance h_c is given by:

$$h_c = \frac{2 k_s n a}{\left(1 - \sqrt{A_r/A_a}\right)^{1.5}} \qquad (1)$$

where $k_s \equiv$ harmonic mean thermal conductivity, $n \equiv$ contact spot density, $a \equiv$ mean contact spot radius and $A_r/A_a \equiv$ ratio of real area to apparent area of contact.

The relationship in the denominator of Eq. (1) accounts for the "crowding" of adjacent microcontacts and it is important for large relative contact pressures.

Table 1 CMY plastic model

Deformation	Results
Plastic	$\frac{A_r}{A_a} = \frac{1}{2} erfc(\lambda/\sqrt{2})$
	$n = \frac{1}{16}\left(\frac{m}{\sigma}\right)^2 \frac{exp(-\lambda^2)}{erfc(\lambda/\sqrt{2})}$
	$a = \sqrt{\frac{8}{\pi}} \frac{\sigma}{m} exp(\lambda^2/2) erfc(\lambda/\sqrt{2})$
	$h_c = \frac{k_s}{2\sqrt{2\pi}} \frac{m}{\sigma} \frac{exp(-\lambda^2/2)}{\left[1 - \sqrt{\frac{1}{2} erfc(\lambda/\sqrt{2})}\right]^{1.5}}$
	$\lambda = \sqrt{2} erfc^{-1}\left(\frac{2P}{H_c}\right)$

Table 2 Mikic elastic model

Deformation	Results
Elastic	$\frac{A_r}{A_a} = \frac{1}{4} erfc(\lambda/\sqrt{2})$
	$n = \frac{1}{16}\left(\frac{m}{\sigma}\right)^2 \frac{exp(-\lambda^2)}{erfc(\lambda/\sqrt{2})}$
	$a = \frac{2}{\sqrt{\pi}}\frac{\sigma}{m} exp(\lambda^2/2) erfc(\lambda/\sqrt{2})$
	$h_c = \frac{k_s}{4\sqrt{\pi}}\frac{m}{\sigma}\frac{exp(-\lambda^2/2)}{\left[1-\sqrt{\frac{1}{4}erfc(\lambda/\sqrt{2})}\right]^{1.5}}$
	$\lambda = \sqrt{2} erfc^{-1}\left(\frac{4\sqrt{2}P}{E'm}\right)$

In Table 1 and Table 2, λ is the dimensionless mean plane separation, σ and m are the surface asperity roughness and slope parameters for the surface pair, P is the applied pressure and E' the equivalent elastic modulus.

The essential differences and similarities between the two models can be summarised as follows:

(i) The ratio $(A_r/A_a)_p = 2\ (A_r/A_a)_e$.
(ii) The contact spot density n is the same.
(iii) The mean contact spot radius $a_p = \sqrt{2}\cdot a_e$.
(iv) The applied pressure P is $[H_c]/2\cdot erfc(\lambda/\sqrt{2})$ and $[(E'/\sqrt{2})\cdot m]/4\cdot erfc(\lambda/\sqrt{2})$ in plastic and elastic deformation respectively.

The elastoplastic model developed here will take into account these differences and it will move smoothly from the elastic model to the fully plastic model.

REVIEW OF DEFORMATION MODELS FOR SPHERE-FLAT CONTACTS

In this section a review of three deformation models for sphere-flat contacts will be presented. The models will be based on two methods of defining surface hardness: i.e., i) hardness based on contact radius or ii) hardness based on contact displacement. These models are connected through simple geometric relationships.

Defining hardness based on circular contact radius (a):

$$H_{d,a} = \frac{\tilde{F}}{\pi a^2} \tag{2}$$

Defining hardness based on contact displacement (δ):

$$H_{d,\delta} = \frac{\tilde{F}}{\pi\beta\delta} \tag{3}$$

where $\tilde{F}$ is the applied load, β is the radius of the spherical indenter and subscript d refers to the type of deformation elastic (e), plastic (p) or elastoplastic (ep).

1. Elastic model of Hertz

A sphere in contact with a flat produces a circular contact. Hertz [Johnson (1985)] solved the problem for an elliptical contact. The circular contact is a special case of the elliptical contact problem. He simplified the problem by assuming that each body can be regarded as an elastic half-space loaded over a small elliptical or circular (in this case) region of its plane surface.

Elastic hardness based on contact radius (a)

The Hertz contact radius "a" in terms of load $\tilde{F}$, geometry β and equivalent elastic modulus E' is given by [see Johnson (1985)]:

$$a = \left(\frac{3\tilde{F}\beta}{4E'}\right)^{1/3} \tag{4}$$

where the equivalent elastic modulus E' is given by:

$$E' = \left(\frac{1-\nu_A^2}{E_A} + \frac{1-\nu_B^2}{E_B}\right)^{-1}$$

where A and B refer to the two surfaces in contact.

From Eq. (4) one obtains

$$\tilde{F} = \frac{4}{3}\cdot\frac{E'a^3}{\beta} \tag{5}$$

Substituting for $\tilde{F}$ in Eq. (2) we have:

$$H_{e,a} = \frac{4}{3\pi}\cdot E'\cdot\frac{a}{\beta} \tag{6}$$

Non-dimensionlising the elastic hardness with the plastic property of material yield/flow stress S_f we have:

$$\frac{H_{e,a}}{S_f} = \frac{4}{3\pi} \cdot \frac{E'}{S_f} \cdot \frac{a}{\beta} = \frac{4}{3\pi} \cdot \epsilon^*_{c,a} \tag{7}$$

where $\epsilon^*_{c,a} = E'/S_f \cdot a/\beta$, $\equiv$ non-dimensional contact strain based on the circular contact spot radius.

Elastic hardness based on contact displacement (δ)

The Hertz contact displacement "δ" in terms of load $\tilde{F}$, geometry β and equivalent elastic modulus E' is given by [see Johnson (1985)]:

$$\delta = \left(\frac{9\tilde{F}^2}{16\beta E'^2} \right)^{1/3} \tag{8}$$

From which one obtains

$$\tilde{F} = \frac{4}{3} \cdot E' \cdot \sqrt{\beta\delta} \cdot \delta \tag{9}$$

Substituting the value of $\tilde{F}$ in Eq. (3) we have:

$$H_{e,\delta} = \frac{4}{3\pi} \cdot E' \cdot \sqrt{\frac{\delta}{\beta}} \tag{10}$$

Non-dimensionlising the elastic hardness with the plastic property of material yield/flow stress S_f we have:

$$\frac{H_{e,\delta}}{S_f} = \frac{4}{3\pi} \cdot \frac{E'}{S_f} \cdot \sqrt{\frac{\delta}{\beta}} = \frac{4}{3\pi} \cdot \epsilon^*_{c,\delta} \tag{11}$$

where $\epsilon^*_{c,\delta} = E'/S_f \cdot \sqrt{\delta/\beta}$, $\equiv$ non-dimensional contact strain based on the contact displacement.

From the Hertz analysis we also have the important geometric relationship:

$$a = \sqrt{\beta\delta} \tag{12}$$

With this result one can obtain the very important relationship between the dimensionless contact strains based on the contact radius or the contact displacement:

$$\epsilon^*_{c,a} = \epsilon^*_{c,\delta} = \epsilon^*_c \tag{13}$$

This result will be used in the development of the elastoplastic model.

2. Geometric plastic model for sphere-flat contact

This simple deformation model assumes that the sphere and the flat interact geometrically under fully plastic deformation. Two forms of plastic hardness model will be considered, i.e., i) contact hardness based on the contact radius and ii) contact hardness based on the contact displacement.

Plastic hardness based on contact radius (a)

The ratio of hardness $H_{p,a}$, to the flow stress S_f under fully plastic deformation is a constant for real strain-hardening materials provided the appropriate value of yield/flow stress S_f is used [Tabor (1951)]:

$$\frac{H_{p,a}}{S_f} = 2.76 \tag{14}$$

where the constant 2.76 is called the plastic constraint factor.

Tabor (1951) suggested a value "2.8" for the plastic constraint factor which was based on experimental observation. Sridhar and Yovanovich (1994) have suggested a value "2.76" which comes from the slip line field model for a rigid punch indenting a rigid plastic material.

Plastic hardness based on contact displacement (δ)

From the geometry of the indentation we can write:

$$a \simeq \sqrt{2\beta\delta} \tag{15}$$

From Eq. (2) we have:

$$H_{p,a} = \frac{\tilde{F}}{\pi a^2} = \frac{\tilde{F}}{2\pi\beta\delta} \tag{16}$$

Therefore

$$\frac{H_{p,\delta}}{S_f} = 5.52 \tag{17}$$

which is twice as large as the ratio based on the contact radius. This is because we chose to define the hardness based on contact displacement in a particular way for convenience.

3. Elastoplastic model for sphere-flat contact

The elastoplastic model for sphere-flat contact was developed by Sridhar and Yovanovich (1994) by "blending" the two asymptotic solutions (elastic and plastic). The elastoplastic model smoothly moves from the elastic asymptote to the plastic asymptote covering the three regimes of loading: elastic, elastoplastic and fully plastic. This model has been validated with data sets from different metals [see Sridhar and Yovanovich

(1993b, 1994)].

This model was presented in two forms; an explicit and an implicit form. In the explicit form the size or displacment of the contact can be directly determined once the applied load and material properties are known. Whereas in the implicit model a numerical technique was required to solve for the contact size or the contact displacement. In this paper only the implicit model is presented below.

Elastoplastic hardness based on contact radius (a)

$$\frac{H_{ep,a}}{S_f} = \frac{2.76}{\left[1+\left(\frac{6.5}{\epsilon^*_{c,a}}\right)^2\right]^{1/2}} \tag{18}$$

We can rewrite the above equation in the following form:

$$\frac{\tilde{F}}{\tilde{A}_{ep}S_f} = \frac{2.76}{\left[1+\left(\frac{6.5}{\epsilon^*_{c}}\right)^2\right]^{1/2}} \tag{19}$$

where $\tilde{A}_{ep}$ is elastoplastic contact area of a single contact spot.

Elastoplastic hardness based on contact displacement (δ)

$$\frac{H_{ep,\delta}}{S_f} = \frac{5.52}{\left[1+\left(\frac{13.0}{\epsilon^*_{c,\delta}}\right)^{1.2}\right]^{1/1.2}} \tag{20}$$

Similarly we have:

$$\frac{\tilde{F}}{\pi\beta\delta S_f} = \frac{5.52}{\left[1+\left(\frac{13.0}{\epsilon^*_{c}}\right)^{1.2}\right]^{1/1.2}} \tag{21}$$

In Eq. (19) and Eq. (21) $\epsilon^*_{c,a}$ and $\epsilon^*_{c,\delta}$ have been replaced by ϵ^*_c because we know that they are equal to each other from Eq. (13).

PRESENT ELASTOPLASTIC MODEL FOR CONFORMING ROUGH SURFACES

From the comparison of the two asymptotic models (Table 1 and Table 2) it is clear that the ratio of real area to apparent area of contact A_r/A_a, size of average contact spot a and the relationship between the applied pressure P and dimensionless mean plane separation λ depend upon the type of deformation. In this section these parameters will be examined and the corresponding expressions for the new elastoplastic model will be derived.

Ratio of real area to the apparent area of contact A_r/A_a

Examining the results of the analyses of the CMY plastic model and the Mikic elastic model we find:

$$4\left(\frac{A_r}{A_a}\right)_{elastic} = 2\left(\frac{A_r}{A_a}\right)_{plastic} = erfc(\lambda/\sqrt{2}) \tag{22}$$

Similarly for a single sphere-flat contact:

$$\tilde{A}_e = \frac{1}{2}\tilde{A}_p = \pi\beta\delta \tag{23}$$

Therefore

$$\frac{\tilde{A}_e}{\tilde{A}_p} = \frac{1}{2} \tag{24}$$

Mikic (1974) derived the ratio A_r/A_a for elastic contact based on Eq. (24) which indicates that the elastic contact area is half that of the plastic contact area.

Elastoplastic contact area for a single contact spot:

From Eq. (19) we have

$$\tilde{A}_{ep} = \frac{\tilde{F}\left[1+\left(\frac{6.5}{\epsilon^*_c}\right)^2\right]^{1/2}}{2.76S_f} \tag{25}$$

Also from Eq. (21) we find

$$\tilde{F} = \frac{5.52\pi S_f\beta\delta}{\left[1+\left(\frac{13.0}{\epsilon^*_c}\right)^{1.2}\right]^{1/1.2}} \tag{26}$$

Substituting for $\tilde{F}$ in Eq. (25) we get:

$$\frac{\tilde{A}_{ep}}{\tilde{A}_p} = \frac{\left[1+\left(\frac{6.5}{\epsilon^*_c}\right)^2\right]^{1/2}}{\left[1+\left(\frac{13.0}{\epsilon^*_c}\right)^{1.2}\right]^{1/1.2}} = f_{ep}(\epsilon^*_c) \tag{27}$$

It will be shown later that ϵ_c^* for conforming rough surfaces in contact is independent of size (a) or displacement (δ) and dependent only on the material properties (E', S_f) and the mean absolute surface slope (m) for a surface pair.

Therefore the elastoplastic ratio of real area to apparent area is given by:

$$\frac{A_r}{A_a} = \frac{f_{ep}(\epsilon_c^*)}{2} erfc(\lambda/\sqrt{2}) \tag{28}$$

It can seen that as $\epsilon_c^* \to 0$, $f_{ep}(\epsilon_c^*) \to 0.5$ and as $\epsilon_c^* \to \infty$, $f_{ep}(\epsilon_c^*) \to 1$. As ϵ_c^* ranges from 0 to ∞, $f_{ep}(\epsilon_c^*)$ moves smoothly from 0.5 to 1.0 as seen in Fig. 1.

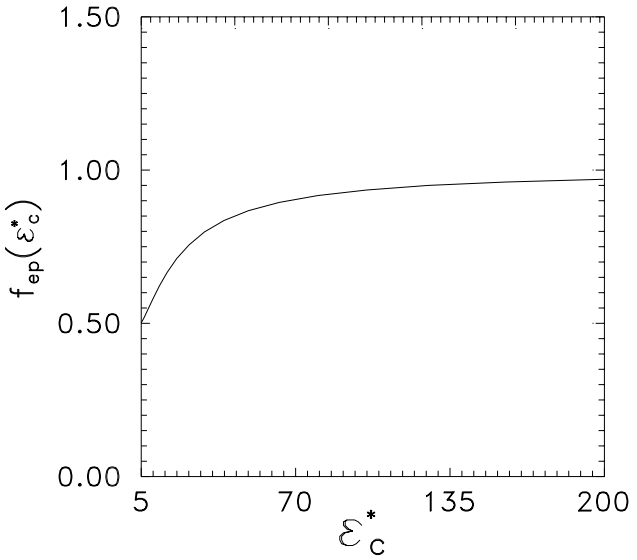

Fig. 1 Plot of the function $f_{ep}(\epsilon_c^*)$ versus ϵ_c^*

Contact spot density n

It can be seen from Tables 1 and 2 that the contact spot density is independent of the type of deformation and remains the same for either the elastic or the plastic deformation.

Therefore for elastoplastic deformation:

$$n = \frac{1}{16}\left(\frac{m}{\sigma}\right)^2 \frac{exp(-\lambda^2)}{erfc(\lambda/\sqrt{2})} \tag{29}$$

Force balance

We know from the CMY plastic model that:

$$\frac{A_r}{A_a} = \frac{P}{H_c} \tag{30}$$

where P $\equiv$ applied pressure and $H_c \equiv$ appropriate contact hardness (plastic) of the softer material.

It was shown by Mikic (1993) for conforming surfaces undergoing elastic deformation that:

$$\frac{A_r}{A_a} = \frac{P}{\frac{E'}{\sqrt{2}}m} = \frac{P}{H_e} \tag{31}$$

Therefore

$$H_e = \frac{E'}{\sqrt{2}} \cdot m \tag{32}$$

where H_e is defined as the elastic hardness of the softer material in contact and m is the mean absolute slope for a surface pair. The elastic hardness H_e refers to the mean pressure on a single mean asperity as it is pressed against a rigid, smooth flat.

Hence we make the assumption that

$$H_e = \frac{E'}{\sqrt{2}} \cdot m = \frac{4}{3\pi} \cdot E' \cdot \frac{a}{\beta} \tag{33}$$

Therefore we find the relationship between the ratio a/β and m:

$$\frac{a}{\beta} = 1.67 \cdot m \tag{34}$$

With this we rewrite ϵ_c^* as:

$$\epsilon_c^* = \frac{E'}{S_f} \cdot \frac{a}{\beta} = 1.67 \cdot \frac{E'}{S_f} \cdot m \tag{35}$$

Finally, we assume for elastoplastic deformation of two conforming rough surfaces in contact that:

$$\frac{A_r}{A_a} = \frac{P}{H_{ep}} \tag{36}$$

where H_{ep} is the elastoplastic hardness given by:

$$H_{ep} = \frac{2.76 S_f}{\left[1 + \left(\frac{6.5}{\epsilon_c^*}\right)^2\right]^{1/2}} \tag{37}$$

Therefore we have

$$\frac{A_r}{A_a} = \frac{f_{ep}(\epsilon_c^*)}{2} erfc(\lambda/\sqrt{2}) = \frac{P}{H_{ep}} \tag{38}$$

and

$$\lambda = \sqrt{2} erfc^{-1}\left(\frac{2}{f_{ep}(\epsilon_c^*)} \frac{P}{H_{ep}}\right) \tag{39}$$

Table 3 summarises the important results of the new elastoplastic model.

Table 3 Elastoplastic model

Results
$\frac{A_r}{A_a} = \frac{f_{ep}(\epsilon_c^*)}{2} erfc(\lambda/\sqrt{2})$
$n = \frac{1}{16}\left(\frac{m}{\sigma}\right)^2 \frac{exp(-\lambda^2)}{erfc(\lambda/\sqrt{2})}$
$a = \sqrt{\frac{8}{\pi}} \cdot \sqrt{f_{ep}(\epsilon_c^*)} \cdot \frac{\sigma}{m} exp(\lambda^2/2) erfc(\lambda/\sqrt{2})$
$h_c = \frac{k_s}{2\sqrt{2\pi}} \frac{m}{\sigma} \frac{\sqrt{f_{ep}(\epsilon_c^*)} \cdot exp(-\lambda^2/2)}{\left[1 - \sqrt{\frac{f_{ep}(\epsilon_c^*)}{2}} erfc(\lambda/\sqrt{2})\right]^{1.5}}$
$\lambda = \sqrt{2} erfc^{-1}\left(\frac{1}{f_{ep}(\epsilon_c^*)} \cdot \frac{2P}{H_{ep}}\right)$

COMPARISON OF THERMAL CONTACT CONDUCTANCE MODELS WITH EXPERIMENTAL DATA

In order to compare the models with themselves as well as with experimental data they have to be cast in dimensionless form. It has been found that the most suitable dimensionless form for contact conductance is:

$$C_c = \frac{\sigma}{m} \cdot \frac{h_c}{k_s} \tag{40}$$

where k_s is the mean harmonic thermal conductivity, σ and m are the equivalent RMS surface roughness and mean absolute slope respectively for a surface pair.

The dimensionless contact pressure used in this work for the three different models are P/H_e, $P/H_{c\ or\ p}$ and P/H_{ep} respectively. where H_e, H_c or H_p and H_{ep} refer to the elastic, the plastic and the elastoplastic hardness respectively.

Table 4 compares the three dimensionless contact conductance models, i.e. the Mikic elastic model, the CMY plastic model and the present elastoplastic model.

It can be seen from Table 4 that as $\epsilon_c^* \to 0$, $f_{ep}(\epsilon_c^*) \to 0.5$ (Fig. 1) and $H_{ep} \to H_e$ (Fig. 2). Similarly as $\epsilon_c^* \to \infty$, $f_{ep}(\epsilon_c^*) \to 1$ (Fig. 1) and $H_{ep} \to H_p$ (or H_c) (Fig. 2).

Figure 3 shows a plot of the new elastoplastic model for different values of the non-dimensional contact strain ϵ_c^*. For $\epsilon_c^* = 0$, the elastoplastic model reduces to the elastic model (Mikic). As ϵ_c^* is increased the elastoplastic model moves downwards. The plots of $\epsilon_c^* = 15$ and 60 are seen to lie below the elastic model but parallel to it. A value of $\epsilon_c^* = \infty$ reduces the elastoplastic model to the plastic model (CMY). It can be seen from Fig. 3 that a single model is able to handle all three regimes of loading, i.e., the elastic, the elastoplastic and the fully plastic.

Table 4 Elastic, plastic and elastoplastic contact conductance models

Deformation	Results
Elastic	$C_c = \frac{1}{4\sqrt{\pi}} \frac{exp(-\lambda^2/2)}{\left[1 - \sqrt{\frac{1}{4} erfc(\lambda/\sqrt{2})}\right]^{1.5}}$ $\lambda = \sqrt{2} erfc^{-1}\left(\frac{4P}{H_e}\right)$
Plastic	$C_c = \frac{1}{2\sqrt{2\pi}} \frac{exp(-\lambda^2/2)}{\left[1 - \sqrt{\frac{1}{2} erfc(\lambda/\sqrt{2})}\right]^{1.5}}$ $\lambda = \sqrt{2} erfc^{-1}\left(\frac{2P}{H_c}\right)$
Elastoplastic	$C_c = \frac{1}{2\sqrt{2\pi}} \frac{\sqrt{f_{ep}(\epsilon_c^*)} \cdot exp(-\lambda^2/2)}{\left[1 - \sqrt{\frac{f_{ep}(\epsilon_c^*)}{2}} erfc(\lambda/\sqrt{2})\right]^{1.5}}$ $\lambda = \sqrt{2} erfc^{-1}\left(\frac{1}{f_{ep}(\epsilon_c^*)} \cdot \frac{2P}{H_{ep}}\right)$

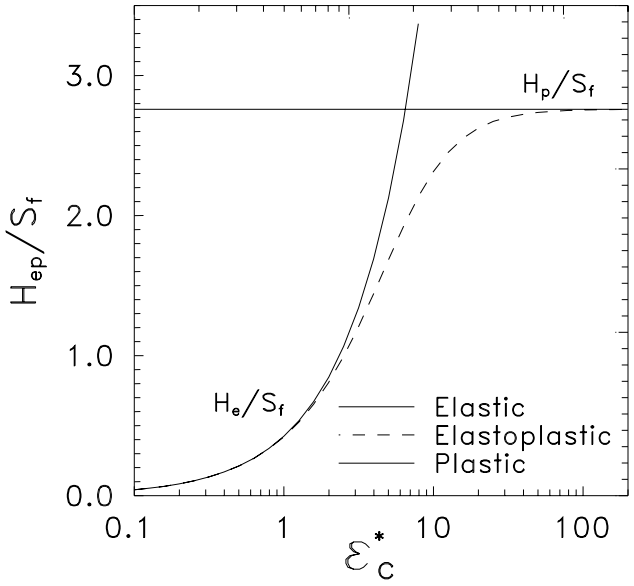

Fig. 2 Elastic, Fully Plastic and Elastoplastic Hardness Models

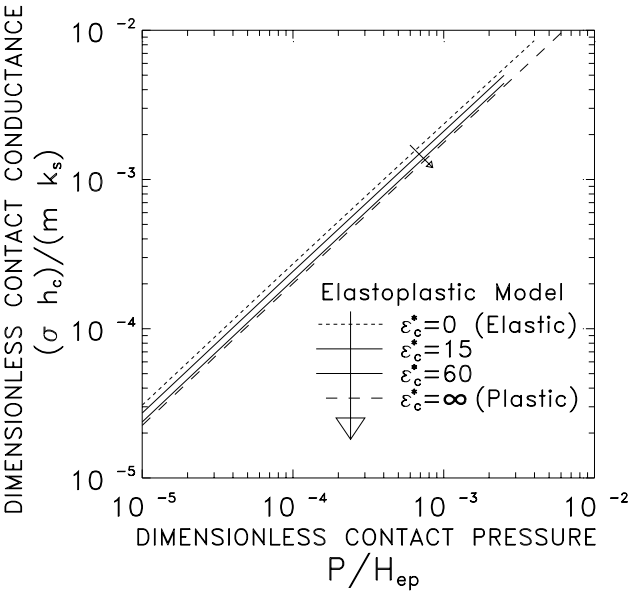

Fig. 3 Plot of the present elastoplastic model for different values of ϵ^*_c

Data reduction

Experimental contact conductance h_c is determined as follows:

$$h_c = \frac{Q}{A_a \Delta T_c} \tag{41}$$

where Q is the heat flow rate, A_a is the apparent contact area and ΔT_c interface temperature drop.

This is non-dimensionlised by multiplying it by $(\sigma/m)/k_s$. The surface parameters σ and m are given by:

$$\sigma = \sqrt{\sigma_A^2 + \sigma_B^2} \tag{42}$$

and

$$m = \sqrt{m_A^2 + m_B^2} \tag{43}$$

where A and B refer to the upper and lower surfaces.

The harmonic mean thermal conductivity k_s is defined as

$$k_s = \frac{2k_A k_B}{k_A + k_B} \tag{44}$$

where k_A and k_B are thermal conductivities of the upper and lower specimens. The thermal conductivities k_A and k_B for a test pair were determined at the mean interface temperature T_c.

Table 5 lists the surface, elastic and plastic properties of all the materials used in this investigation.

The data sets used in the present study cover a wide range of thermal, material and surface properties. Data obtained for isotropic surface pairs by Antonetti (1983) and Hegazy (1985) cover a wide range of pressures ranging from 0.4 *MPa* to 8.9 *MPa*. The elastic modulus varied from 96 *GPa* for the Zirconium alloys to 207 *MPa* for Ni200 and SS304. The data also covered a wide range of surface roughness ($6 < \sigma/m < 60\ \mu m$) , mean interface temperatures ($108 < T_c < 175\ ^\circ C$) and thermal properties ($16 < k_s < 77\ W/m \cdot K$).

The microhardness in column 5 of Table 5 is an elastoplastic property of a material and in the case of microhardness measurements it is dependent on the size of indentation d_V called the Vickers indentation diagonal. Hence the Vickers microhardness appears as a correlation between Vickers microhardness H_V and the size of indentation d_V. They were obtained by performing careful microhardness tests on the softer material in contact.

Iterative procedure to determine P/H_{ep}

From the experimental correlations of microhardness it is clear that it is dependent on the size of indentation. This is because the surface machining produces surface layers which are harder than the bulk. In order to determine the dimensionless contact pressure P/H_{ep}

for each experimental point one has to know the appropriate value of elastoplastic contact microhardness H_{ep}. An iterative technique was required to determine this appropriate elastoplastic contact microhardness. The technique used in the present work is similar to the one developed by Yovanovich et al. (1982), Yovanovich et al. (1983) and Yovanovich and Hegazy (1983). The only difference is that the elastoplastic model is used instead of the fully plastic model (CMY).

Table 5 Test pairs, surface and material characteristics

Material	$\frac{\sigma}{m}$ μm	E GPa	ν	Vickers microhardness $H_V = c_1 {d_V}^{c_2}$ GPa
Ni200	08.20* 08.81** 17.86** 18.01** 18.05* 22.55* 24.62** 41.80* 59.83*	207	0.3	$^*H_V = 6.304 d_V^{-0.264}$
SS304	06.64* 23.36* 40.27* 57.63*	207	0.3	$^*H_V = 6.271 d_V^{-0.229}$
Zr-Nb	11.11* 15.43* 32.55* 44.05*	96	0.3	$^*H_V = 5.884 d_V^{-0.267}$
Zr-4	12.43* 18.58* 24.34* 38.26*	96	0.3	$^*H_V = 5.677 d_V^{-0.278}$

* Hegazy (1985), ** Antonetti (1983)

Examining the expression for the elastoplastic hardness, Eqs. (35), (37), it can be seen that the value of yield/flow stress S_f is unknown. Hence an appropriate value of S_f has to be chosen in order to determine the elastoplastic hardness H_{ep}. The iterative procedure developed calculates the appropriate value of S_f and thus the elastoplastic hardness H_{ep}.

Equations (45) through (51) constitute the present model for predicting P/H_{ep} for a particular applied pressure P on a conforming rough surface pair. The expression for S_f in Eq. (51) was obtained by solving for S_f using Eq. (37).

$$H_{ep} = \frac{H_V}{0.9272} = \frac{c_1}{0.9272} \cdot {d_V}^{c_2} \tag{45}$$

$$d_V = \sqrt{2\pi} \cdot a \tag{46}$$

$$a = \sqrt{\frac{8}{\pi}} \cdot \sqrt{f_{ep}(\epsilon_c^*)} \cdot \frac{\sigma}{m} exp(\lambda^2/2) erfc(\lambda/\sqrt{2}) \tag{47}$$

$$\lambda = \sqrt{2}\ \ erfc^{-1}\left(\frac{1}{f_{ep}(\epsilon_c^*)} \cdot \frac{2P}{H_{ep}}\right) \tag{48}$$

$$f_{ep}(\epsilon_c^*) = \frac{\left[1 + \left(\frac{6.5}{\epsilon_c^*}\right)^2\right]^{1/2}}{\left[1 + \left(\frac{13.0}{\epsilon_c^*}\right)^{1.2}\right]^{1/1.2}} \tag{49}$$

$$\epsilon_c^* = 1.67\ \ \frac{E'}{S_f} \cdot m \tag{50}$$

$$S_f = \frac{1}{2.76\sqrt{\frac{1}{H_{ep}^2} - \frac{1}{H_e^2}}} \tag{51}$$

In Eq. (45) the Vickers microhardness H_V is divided by 0.9272 to convert the Vickers hardness which is based on total surface area of indentation to a hardness which is based on the projected area. This is because hardness is defined based on the projected area of indentation.

The above set of Eqs. (45) through (51) were solved iteratively using *Mathematica* (1988-91) until the assumed value of H_{ep} in Eq. (51) and the calculated value of H_{ep}, Eq. (45) coincided. The numerical "FindRoot" was used to achieve this. The "FindRoot" command in *Mathematica* (1988-91) required two guesses around the actual root. One guess was 0.9 H_e and an another equal to the value of the bulk hardness of the material was

used. If the elastoplastic hardness is equal to the elastic hardness then the iterative procedure appears to fail. This problem can be avoided by setting the yield/flow stress S_f equal to ∞ in Eq. (51). Then ϵ_c^* in Eq. (50) will go to zero and $f_{ep}(\epsilon_c^*)$, Eq. (49), will go to 0.5 and H_{ep} reduces to H_e (Eq. (48)) and so on, i.e., the elastoplastic model reduces to the elastic model.

Comparison of experimental data with the proposed models

It was clear from the iterative procedure that each surface pair depending upon its surface and material characteristics will have different values of ϵ_c^*. It was found that the value of ϵ_c^* was almost invariant for a single surface pair and as load was increased it remained more or less constant. The non-dimensional strain ϵ_c^* used in the elastoplastic model is strongly dependent on the value of surface slope m. It is known that this quantity (m) is difficult to measure without errors. The extent of care taken during the measurement of surface slope m by previous researchers is not clear. Hence at this stage the experimental data from Antonetti (1983) and Hegazy (1985) will be reduced to a dimensionless form using the elastoplastic model and compared with the two asymptotes, i.e., the elastic ($\epsilon_c^* = 0$) and plastic models ($\epsilon_c^* = \infty$). Ideally data should lie between these two bounds, i.e., the Mikic elastic model and CMY plastic model. The asymptotes run parallel to each other and are quite close (difference $\simeq$ 40 %). It should be noted that in the past data could not be compared with both the elastic and plastic models because a type of deformation had to be assumed *a priori*.

Figure 4 shows the comparison of experimental data from Antonetti (1983) and Hegazy (1985) for Ni200 conforming rough surface pairs with the elastic model and the plastic models. The data set covers a wide range surface roughness with the roughness parameter σ/m varying from 8.2 μm to 59.8 μm. Even though the light load data points show some scatter the data lie well within the bounds set by the elastic and plastic models. The value of ϵ_c^* determined for each load using the proposed iterative procedure in this paper varied from 12.0 for the smoothest surface to 53.0 for the roughest one.

Figure 5 shows the comparison between the SS304 data from Hegazy (1985) with the elastic and the plastic models. The four surface pairs covered a range of roughness values with σ/m varying from 6.6 to 57.6 μm. Most of the data lie between the two bounds set by the elastic and plastic models. However there are some data points at the low contact pressures which lie outside the bounds. The value of ϵ_c^* varied from 4.0 to 36.0 for the SS304 data sets shown in Fig. 5.

Figure 6 shows the comparison between the Zr-Nb data from Hegazy (1985) with the elastic, and plastic models. The low load data points lie outside the bounds of the elastic and plastic models. However, the data points at higher loads lie within the bounds. This material was found to be quite elastic in comparison to Ni200 and SS304. The proposed iterative scheme recommends a value of ∞ for yield/flow stress S_f for the smoothest pair ($\sigma/m = 11.1\ \mu m$), which means that ϵ_c^* = 0. The value ϵ_c^* varied from 9.0 to 20.0 for the other pairs.

Figure 7 shows another Zirconium alloy Zr-4 compared with the elastic and the plastic models. The smoothest pair underwent predominantly elastic deformation. This data set lies outside the lower bound, i.e., the plastic model. For the other pairs (σ/m ranged from 18.6 to 38.3), ϵ_c^* varied from 9.0 to 21.0. These data sets lie slightly outside the bounds closer to the elastic model.

DISCUSSION AND CONCLUDING REMARKS

The non-dimensional strain $\epsilon_c^* = 1.67\ (E'/Sf) \cdot m$ is similar to the plasticity index proposed by Mikic (1974) except that the hardness H is replaced by a yield/flow stress S_f and a constant (1.67) appears here. This non-dimensional strain is a combination of both the material and surface properties of a particular pair.

The comparison of the two asymptotic models (elastic and plastic) with Ni200, SS304 and Zr-Nb data from Antonetti (1983) and Hegazy (1985) is excellent. The Ni200 data show significant plastic deformation with ϵ_c^* varying from 12.0 to 36.0. The smoothest pair of SS304 shows significant elastic deformation with a value of ϵ_c^* = 4.0. The remainder of the SS304 pairs show fair amount of plastic deformation with ϵ_c^* varying from 16.0 to 36.0.

The two Zirconium alloys Zr-Nb and Zr-4 show significant elastic deformation and the maximum value of ϵ_c^* for the roughest pair is only 21.0. The smoothest pairs in both materials underwent predominantly elastic deformation. The comparison of the Zr-4 data of the smoothest pair with the models is not satisfactory. This maybe due to the errors in surface slope or hardness measurements.

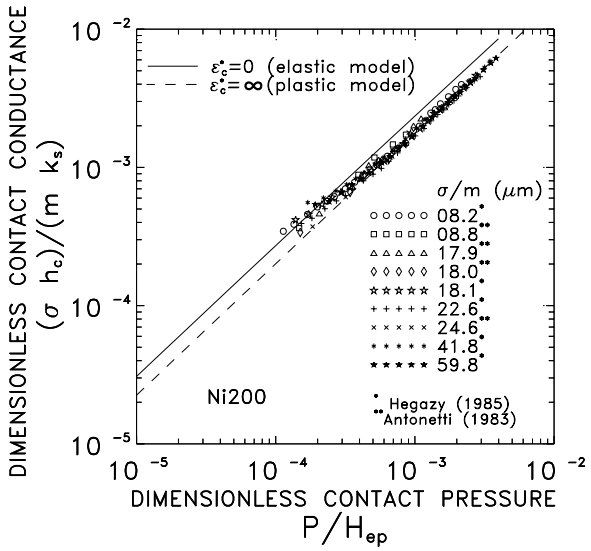

Fig. 4 Comparison of elastic and plastic asymptotic models with Ni200 data [Hegazy (1985) and Antonetti (1983)] reduced using the proposed elastoplastic model

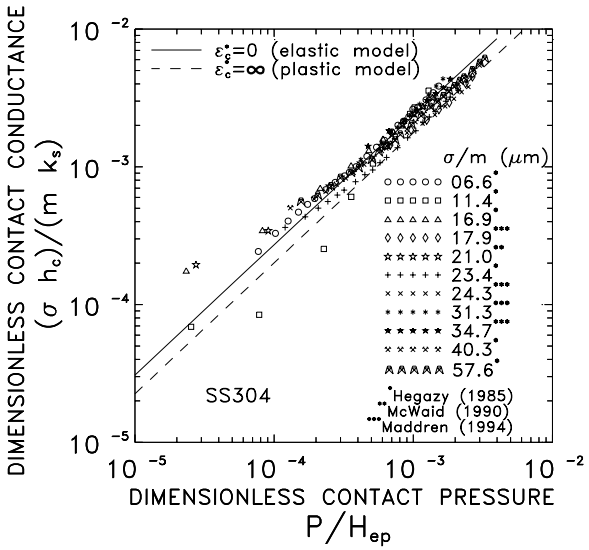

Fig. 5 Comparison of elastic and plastic asymptotic models with SS304 data [Hegazy (1985)] reduced using the proposed elastoplastic model

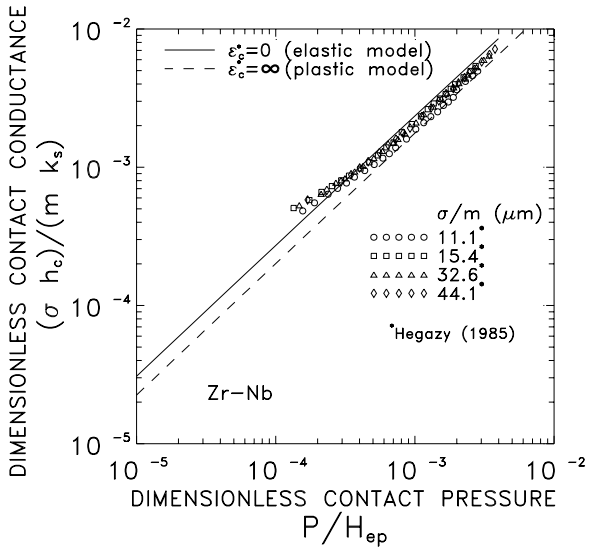

Fig. 6 Comparison of elastic and plastic asymptotic models with Zr-Nb data [Hegazy (1985)] reduced using the proposed elastoplastic model

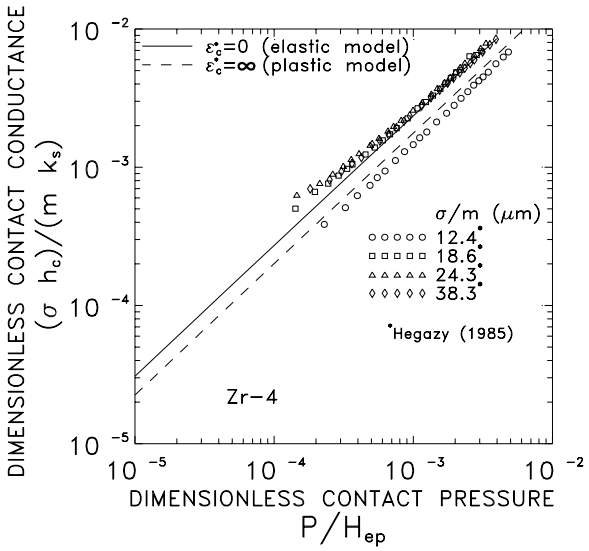

Fig. 7 Comparison of elastic and plastic asymptotic models with Zr-4 data [Hegazy (1985)] reduced using the proposed elastoplastic model

For the first time thermal contact conductance data have been reduced using an elastoplastic model and compared with both the elastic and plastic models on the same plot. The elastoplastic model eliminates the dilemma of assuming a type of deformation *a priori*.

Most of the data sets from Hegazy (1985) and Antonetti (1983) lie within the two bounds set by the elastic and plastic models, which indicates the merit of using the present elastoplastic model to reduce the data.

Surface slope m is an important parameter of the elastoplastic model and there is a need to determine this accurately. At this stage it is believed that the discrepancies between some data and the model are due to errors in the value of the surface slope. Future work should be aimed at obtaining a better estimate of the surface slope m.

ACKNOWLEDGMENTS

The authors acknowledge the support of the Natural Science and Engineering Research Council of Canada under grant A7445.

REFERENCES

Antonetti, V. W., 1983, "On the Use of Metallic Coatings to Enhance Thermal Contact Conductance," Ph.D. Thesis, University of Waterloo, Canada,

Bush A. W., Gibson R. D., and Thomas T. R., 1975, "The Elastic Contact of a Rough Surface," *Wear,* 35, pp. 87-111.

Chang, W. R., Etsion, I., and Bogy, D. B., 1987, "An Elastic-Plastic Model for the Contact of Rough Surfaces," ASME Journal of Tribology, Vol. 109, pp. 257-263.

Cooper, M. G., Mikic, B. B., and Yovanovich M. M., 1969, "Thermal Contact Conductance," *Int. J. Heat Mass Transfer*, Vol. 12, pp. 279-300.

Fisher, N.J., 1985, "Analytical and Experimental Studies of the Thermal Contact Resistance of Sphere/Layered Flat Contacts," M.A.Sc. Thesis, University of Waterloo, Canada.

Foss, F. E. and Brumfield, R.C., 1922, "Some Measurements of the Shape of Brinell Ball Indentation," Proceedings, ASTM, Vol. 22, p. 312.

Greenwood, J. A., and Williamson, J. B. P., 1966, "Contact of Nominally Flat Surfaces," *Proc. Roy. Soc. Lond.,* A295, pp. 300-319.

Hegazy, A. A., 1985, "Thermal Joint Conductance of Conforming Rough Surfaces," Ph.D. Thesis, University of Waterloo, Canada.

Ishigaki, H., Kawaguchi, I., and Mizuta, S., 1979, "A Simple Estimation of the Elastic-Plastic Deformation of Contacting Asperities," Wear, Vol. 54, pp. 157-164.

Johnson, K. L., 1985, *Contact Mechanics*, Cambridge University Press, Cambridge, Cambridge.

Majumdar, A., and Bhushan, B., 1991, "Fractal Model of Elastic-Plastic Contact Between Rough Surfaces," *ASME Journal of Tribology,* Vol. 113, pp. 1-11.

Mikic, B. B., and Roca, R.T., 1993, "On Elastic Deformation of Rough Surfaces in Contact," *Unpublished Work*, through personal communication from Mikic, B.B. to Yovanovich, M.M..

Mikic, B. B., 1974, "Thermal Contact Conductance; Theoretical Considerations," *Int. J. Heat Mass Transfer*, Vol. 17, pp. 205-214.

Mathematica, 1988-91, *A System for Doing Mathematics by Computer*, Version 2.2 for DOS, Wolfram Research, Inc., Champaign, Illinois.

Sridhar, M. R., and Yovanovich M. M., 1993a, "Critical Review of Elastic and Plastic Thermal Contact Conductance Models and Comparison with Experiment," AIAA-93-2776, AIAA 28th Thermophysics Conference, July 6-9, Orlando, Florida.

Sridhar, M. R., and Yovanovich M. M., 1993b, "Elastoplastic Constriction Resistance of Sphere/Flat Contacts: Theory and Experiment," HTD-Vol. 263, Enhanced Cooling Techniques for Electronics Applications, ASME Winter Annual Meeting, Nov 28-Dec 3, New Orleans, Lousiana.

Sridhar, M. R., and Yovanovich M. M., 1994, "Elastoplastic Model for Indentation of Annealed to Fully Work-Hardened Half-Spaces by a Frictionless Elastic Sphere," paper under preparation.

Tabor, D., 1951, *The Hardness of Metals*, Oxford University Press, London.

Whitehouse, D. J., and Archard, J. F., 1970, "The Properties of Random Surfaces of Significance in their Contact", *Proc. Roy. Soc. Lond.*, A316, pp. 97-121.

Yovanovich, M. M., 1982, "Thermal Contact Correlations", Spacecraft Radiative Transfer and Temperature Control," Edited by T.E. Horton, Vol. 83 of Progress in Astronautics and Aeronautics, New York.

Yovanovich, M. M., Hegazy, A. A., and De Vaal, J., 1982, "Surface Hardness Distribution Effects Upon Contact, Gap and Joint Conductances," AIAA Paper No. 82-0887, AIAA/ASME 3rd Joint Thermophysics, Fluids, Plasma and Heat Transfer Conference, June 7-11, St. Louis, Missouri.

Yovanovich, M. M., Hegazy, A. A., and Antonetti, V. W., 1983, "Experimental Verification of Contact Conductance Models Based Upon Distributed Surface Micro-hardness," AIAA Paper No. 83-0532, AIAA 21st Aerospace Sciences Meeting, January 10-13, Reno, Nevada.

Yovanovich, M. M., and Hegazy, A. A., 1983, "An Accurate Universal Contact Conductance Correlation for Conforming Rough Surfaces with Different Micro-Hardness Profiles", AIAA Paper No. 83-1434, AIAA 18th Thermophysics Conference, June, Montreal, Canada.